Study of Signal Estimation Parameters via Rotational Invariance Technique by Using Ants Colony Optimization Algorithm

Ali Abdul-Elah Noori*, Sadiq Kamel Gharghan* & Ali Jaber Abdul Wahhab*

Received on:30/6/2010
Accepted on:3/2/2011

Abstract

In this paper, an algorithm based on Ants Colony Optimization (ACO) is proposed for extraction of the Directions of Arrival (DOA) of several signals impinging on uniform linear arrays. This algorithm is used to reduce the computation time and complexity that occur in Estimation of Signal Parameters via Rotational Invariance Technique (ESPRIT). In order to illustrate the accuracy and flexibility of the proposed algorithm, several simulation cases introduce of ESPRIT-DOA estimation by using ACO algorithm in environment of Matlab 7.8 program. Results are statistically analyzed in order to conclude from it the algorithm's accuracy and reliability.

Keywords: Direction of Arrival (DOA); Estimation of Signal Parameters via Rotational Invariance Technique (ESPRIT); Ants Colony Optimization (ACO) algorithm.

دراسة تقنية تخمين ثوابت الاشارة بواسطة التعاقب اللا متغير باستخدام خوارزمية مستعمرة النمل

الخلاصة

تُقترح في هذا البحث خوارزمية معتمدة على ايجاد الحل الامثل بواسطة مستعمرة النمل لاستخراج اتجاهات الوصول لإشارات متعددة ساقطة على مصفوفة الهوائيات الخطية المنتظمة. تستعمل هذه الخوارزمية لتقليل الوقت الحسابي والتعقيد الذي يحدث في تقنية تخمين ثوابت الاشارة بواسطة التعاقب اللا متغير. لكي تُوضح الدقةَ ومرونةَ الخوارزميةِ المُقتَرحة, تُقدم عدة حالات محاكاةٍ من تقنية تخمين ثوابت الاشارة بواسطة التعاقب اللا متغير من اتجاهات الوصول باستخدام خوارزمية مستعمرة النمل في بيئة برنامج Matlab 7.8. تم تحليّل النتائج بشكل إحصائي لكي تستنتج منها دقة الخوارزمية والوثوقية.

1. Introduction

Direction-of-arrival (DOA) estimation of narrow-band signals is a fundamental problem in many sensor array systems such as radar, sonar, mobile communications, radio astronomy, and etc. Estimating the direction-of-arrival of impinging waves for antenna-array receivers is a very useful tool for spatially separating sources in multiuser communication systems. Some DOA standard techniques, such as estimation of signal parameters via rotational invariance technique (ESPRIT) [1,2]. The ESPRIT achieves accurate DOA estimates without full

* College of Electrical and Electronic Techniques/ Baghdad

knowledge of antenna array response (no measurement or storage of calibration data is necessary), and because ESPRIT has a very modular implementation involving only repeated low-order eigen-decomposition, the algorithm is especially well-suited to real-time scenarios. Though ESPRIT works well in most cases, ESPRIT has two major problems related to its implementation and performance. First, the method requires a procedure to map the subband spatial frequency back to the full band. This manipulation is necessary because of the widening of the spatial frequency spacing. Second, the reduction of computational load in the singular value decomposition (SVD) is achieved at the expense of compromising the output SNR [3].

It is well known that the classical optimization techniques are likely to be stuck in local minima if the initial guesses are not reasonably close to the final solution. The most of the classical optimization techniques and analytical approaches also suffer from the lack of producing flexible solutions for a given
antenna pattern synthesis problem. The disadvantages of the classical and analytical techniques and rapid envelopment of computer technologies in recent years have encouraged the researcher to use the evolutionary optimization algorithms based on computational intelligence methodologies. It was shown that the evolutionary optimization techniques such as the Ant Colony Optimization (ACO) [4] Genetic Algorithm (GA) [5] and Differential Evolution Algorithm (DEA) [6] are capable of performing the better and more flexible solutions than the classical optimization techniques and the conventional analytical approaches.

The ACO is a paradigm for designing metaheuristic algorithms for combinatorial optimization problems. The first algorithm which can be classified within this framework was presented in 1991 [7, 8] and, since then, many diverse variants of the basic principle have been reported in the literature. The essential trait of ACO algorithms is the combination of a priori information about the structure of a promising solution with a posteriori information about the structure of previously obtained good solutions. The ACO has some distinguished features. It operates on a population of points in search space simultaneously, not on just one point, does not use the derivatives or any other information, and employs probabilistic transition rules instead of deterministic ones. It also has the ability of getting out local minima. As a relatively novel optimization algorithm, the ACO has been successfully applied to solve various engineering problems [9-12].

2. System Model And Problem Formulation

Let uniform linear array be composed of M identical elements, which receive the impinging from directions θ_1, θ_2,.., θ_V narrow-band signals emitted by V far-field sources as shown in Fig. (1).

From the measured output of array the objective is to estimate the sources DOAs. The $M \times 1$ array output vector can be expressed as

$$x(t) = A(\theta)s(t) + n(t) \qquad (1)$$

where $A(\theta) = [a(\theta_1, \ldots, a(\theta_V)]$ is the $M \times V$ matrix of the source steering vectors, $a(\theta)$ is the

$M \times 1$ steering vector, $s(t)$ is the $V \times 1$ vector of source complex envelopes, $n(t)$ is the $M \times 1$ vector of sensor noise. The number of sources V is assumed to be known. Also is assumed, that source signals are zero-mean, complex Gaussian, temporally white processes with the covariance matrix $S = E[s(t)s^H(t)]$, where $E[.]$ and $(.)^H$ stand for expectation operator and hermitian transpose, respectively. The sensor noise $n(t)$ is also the zero-mean complex Gaussian process and is assumed to be both temporally and spatially white with the variance σ^2. Let R denote the covariance matrix of $x(t)$. In accordance with the made assumptions, R is given by

$$R = E[x(t)x^H(t)] = A(\theta)SA^H(\theta) + \sigma^2 I \quad (2)$$

where I is the $M \times M$ identity matrix. The sample covariance matrix obtained from N snapshots is determined as

$$\hat{R} = \frac{1}{N}\sum_{t=1}^{N} x(t)x^H(t) \quad (3)$$

The eigen-decomposition of $\hat{R}$ has the following form

$$\hat{R} = \hat{E}_S \hat{\Lambda}_s \hat{E}_S^H + \hat{E}_n \hat{\Lambda}_n \hat{E}_n^H \quad (4)$$

where $\hat{V} \times \hat{V}$ and $(M - \hat{V}) \times (M - \hat{V})$ diagonal matrices $\hat{\Lambda}_s$ and $\hat{\Lambda}_n$ contain $\hat{V}$ and $M - \hat{V}$ signal and noise subspace eigen-values, whereas $M \times \hat{V}$ matrix $\hat{E}_S = [\hat{e}_1, \ldots. \hat{e}_{\hat{V}}]$ and $M \times (M - \hat{V})$ matrix $\hat{E}_n = [\hat{e}_{\hat{V}+1}, \ldots. \hat{e}_{\hat{V}+1}]$ contain the corresponding eigenvectors, i.e. signal - and noise - subspace eigenvectors.

When realizing the ESPRIT algorithm the selection matrices $J_1 = [I_{m\times m} \; 0_{m\times 1}]$ and $J_2 = [O_{m\times 1} \; I_{m\times m}]$ are formed, where $0_{m\times 1}$ is the zero matrix of size $m \times 1$, m is the number of elements at each subarray and in the maximum overlapping case $m = M - 1$. In [13] more fully exploits the ULA structure by reason of using more than one subarray pairs (but subarray is of smaller size) is proposed. This is accomplished by means of corresponding selection matrices $J_{1s} = [\bar{J}_{q\times m} \; 0_{q\times 1}]$ and $J_{2s} = [0_{q\times 1} \; \bar{J}_{q\times m}]$, where $q = m_s(M - m_s)$ is the total number of elements in each subarray for this case,

$\bar{J} = [\bar{J}^T_1, \bar{J}^T_2, \ldots, \bar{J}^T_{M-m_s}]$,

$\bar{J}_i = [0_{m_s\times(i-1)} \; I_{m_s\times m_s} \; 0_{m_s\times(M-1-m_s)}]$

and $(.)^T$ denote transpose. Here m_s is the number of elements in a subarray of smaller size ($m_s < m$). In this case $m_s \times m$, matrix $\bar{J}_i$ picks m_s contiguous rows of the matrix E_s: $i, i+1, \ldots i + m_s - 1$. This overlapping is named in [6] as generalized and obviously that a choice of $m_s = 1$ leads back to the initial overlapping structure.

In the ESPRIT algorithm with generalized overlapping under estimation of DOAs the eigen-decomposition of the following matrix multiplication is calculated

$$[J_{1s}E_sJ_{2s}]^H[J_{1s}E_sJ_{2s}E_s] = [J_1E_sJ_2E_s]^H\Sigma[J_1E_sJ_2E_s] \quad (5)$$

where $\Sigma = \bar{J}^T\bar{J}$ is the $(M-1)\times(M-1)$ weighting matrix. At this point instead of both immediate using of matrices J_{1s}, J_{2s} and work with the left side of (5) it is appropriate to use the right side of (5). The matrix Σ is the diagonal,

$\Sigma = diag[1\ 2 \ldots. w \ldots. w \ldots .2\ 1], w = \min(m_s, M - m_s)$

. As for parameter m_s, it under maximum overlapping of subarrays in [13] is recommended $m_s \approx (\frac{M}{2})$. The elements of the matrix Σ indicate how many times each row of matrix A is used (in other words, how many times the every element of first subarray of size $M-1$ in a subarray pairs is used).

The useful property of array with symmetrical arrangement of identical in pairs sensors consists in that if to take the array center as phase reference, then the source steering vector will of the conjugate-centrosymmetric form [14]:

$$\bar{a}(\omega) = [\exp\left(-j\left(\frac{M-1}{2}\right)\omega\right), exp\left(-j\left(\frac{M-3}{2}\omega\right)\right),\ldots \ldots exp\left(j\left(\frac{M-3}{2}\omega\right)\right), exp\left(j\left(\frac{M-1}{2}\omega\right)\right)]^T \quad (6)$$

Where $\omega = 2\pi sin\theta/\lambda$ is a so called spatial frequency, d is the interelement spacing, λ is the wave length. Under using of the unitary transformation method the complex-valued vector $\bar{a}(\omega)$ is transformed into real-valued vector $d(\omega) = U^H\bar{a}(\omega)$ of the same size by the matrix

$$U_{2K+1} = \left(\frac{1}{\sqrt{2}}\right)\begin{bmatrix} I_K & 0 & jI_K \\ 0^T & \sqrt{2} & 0^T \\ \tilde{I}_k & 0 & -j\tilde{I}_k \end{bmatrix} \quad (7)$$

if $M = 2K+1$ (i.e. the number of sensors is odd), where matrix $\tilde{I}_k$ is an $(M-1)/2 \times (M-1)/2$ exchange matrix (with ones on its antidiagonal and zeros elsewhere) and by matrix U_{2K} , which is obtained from (7) by dropping its center row and center column, for the case of $M = 2K$.

The source steering vector satisfies the shift invariance property [15], that for the generalized overlapping is expressed as

$$\exp(j\,\omega)J_{1s}\bar{a}(\omega) = J_{2s}\bar{a}(\omega) \quad (8)$$

Since $M \times M$ matrix U is unitary, this leads $U^HU = I$, then (8) may be presented as

$$\exp(j\,\omega)J_{1s}Ud(\omega) = J_{2s}Ud(\omega) \quad (9)$$

Premultiplying both sides of the above mentioned expression by $q \times q$ matrix $U^H{}_q$, we obtain the following formula

$$\exp(j\,\omega)U^H{}_qJ_{1s}Ud(\omega) = U^H{}_qJ_{2s}Ud(\omega) \quad (10)$$

Note, that matrix U_q is formed analogously to the matrix U by (7), and matrices J_{1s} and J_{2s} satisfy the equality $\tilde{I}_qJ_{2s}\tilde{I} = J_{1s}$, where $\tilde{I}_q$ and $\tilde{I}$ are exchange matrices of sizes $q \times q$ and $M \times M$, respectively. As a result, we have

$$U^H{}_qJ_{2s}U = U^H{}_q\tilde{I}_q\tilde{I}_qJ_{2s}\tilde{I}\,\tilde{I}U = U^T{}_qJ_{1s}U^* = (U^T{}_qJ_{1s}U)^* \quad (11)$$

Mark the real and imaginary parts of matrix multiplication $U^H{}_qJ_{2s}U$ as K_{1s} and K_{2s} (they are $q \times M$ real-valued matrices):

$$K_{1s} = Re(U^H{}_qJ_{2s}U), K_{2s} = Im(U^H{}_qJ_{2s}U) \quad (12)$$

According to this definition, (10) may be presented as

$$\exp(j\,\omega)(K_{1s} - jK_{2s})d(\omega) = \exp(-j\,\omega/2)(K_{1s} + jK_{2s})d(\omega) \quad (13)$$

After simple manipulations the following expression can be obtained

$$tg\left(\frac{\omega}{2}\right)K_{1s}\,d(\omega) = K_{2s}\,d(\omega) \quad (14)$$

Let us define the transformed steering matrix as $D = U^H\bar{A}$. Then for all $\hat{V}$ sources the real-valued relation (14) may be expressed as

$$K_{1s}\, D\Omega_{\omega} = K_{2s}\, D \quad (15)$$

where $\Omega_{\omega} = diag[\tan\left(\frac{\omega_i}{2}\right)]_{i=1}^{V}$ cont ains the desired information about DOAs, $D = [d(\omega_1), \ldots., d(\omega_{\hat{V}})]$.

It should be noted, that analogously to ESPRIT with structure weighting in this case is necessary to calculate eigen-decomposition of matrix multiplication

$$[K_{1s}\, E_{su} K_{2s}\, E_{su}]^H [K_{1s}\, E_{su} K_{2s}\, E_{su}] = [K_1\, E_{su} K_2\, E_{su}]^H U^H{}_{M-1} \sum U_{M-1} [K_1\, E_{su} K_2\, E_{su}] \quad (16)$$

where matrix $\hat{E}_{su}$ consists of signal-subspace eigenvectors of matrix $Re\left(U^H \hat{R} U\right), K_1 = Re(U^H{}_{M-1} J_2 U), K_2 = Im(U^H{}_{M-1} J_2 U)$,

and obtained weighting matrix $U^H{}_{M-1} \sum U_{M-1} = \sum un$ is also diagonal, such that $\sum un = diag[1\ 2\ \ldots w\ w\ 1\ 2\ \ldots w]$.

3. Esprit Algorithm

A sequence of steps for realization of the unitary ESPRIT algorithm with structure weighting and maximum overlapping is as follows:

1. computation of the ED of matrix $Re\left(U^H \hat{R} U\right)$ and obtaining of $M \times \hat{V}$ matrix $\ddot{E}_{su}$, whose columns are eigenvectors of $Re\left(U^H \hat{R} U\right)$, that correspond to the $\hat{V}$ greatest eigen-values of $Re\left(U^H \hat{R} U\right)$;
2. definition of $(M-1) \times M$ matrices K_1, K_2 , and calculation of the ED of matrix multiplication $[K_1 E_{su} K_2 E_{su}]^H U^H{}_{M-1} \sum U_{M-1} [K_1 E_{su} K_2 E_{su}] = E_o \Lambda E^H{}_o$,where Λ is the eigen-value matrix of this multiplication, and E_o is the eigenvector matrix ;
3. partition of the matrix E_o into submatrices of size $\hat{V} \times \hat{V}$ $E_o = \begin{bmatrix} E_{11} & E_{12} \\ E_{21} & E_{22} \end{bmatrix}$
4. calculation of the eigen-values $\lambda_V, V = 1, \ldots., \hat{V}$ of matrix $\Psi, \Psi = (-E_{12} E_{22}^{-1})$;
5. determination of the spatial frequency sources as $\omega = 2\tan(\lambda_i), i = 1, \ldots \hat{V}$.

4. Ant Colony Optimization Algorithm

The Ant Colony Optimization (ACO) was firstly proposed by Dorigo and *et al.* for the combinatorial optimization problem solving [16], and numerous variations have been studied ever since. It is an efficient method for handling various optimization tasks, such as routing and scheduling [17-19]. The ACO can be characterized by [20]:

(1) Probabilistic transition rule is used to determine the moving direction of each ant,

(2) Pheromone update mechanism indicates the problem solution quality.

Local search is indeed important in dealing with continuous optimization problems. The continuous ACO has been extended to a hierarchical structure, in which the global search only aims at the 'bad' regions of the search space, while the goal of local search is to exploit those 'good' regions. The basic ACO algorithm for continuous optimization at each generation is described as follows [20].

a. Create n_r global ants.
b. Evaluate their fitness.
c. Update pheromone and age of weak regions.

d. Move local ants to better regions, if their fitness is improved. Otherwise, choose new random search directions.
e. Update ants' pheromone.
f. Evaporate ants' pheromone.

Obviously, the continuous ACO is based on both the global and local search towards the elitist. The local ants have the capability of moving to the latent region with the best solution, according to transition probability $P_i(t)$ of region:

$$P_i(t) = \frac{\tau_i(t)}{\sum_{j=1}^{g} \tau_j(t)} \quad (17)$$

where $\tau_i(t)$ is the total pheromone at region i at time t, and g is the number of global ants. Therefore, the better the region is, the more attraction to the successive ants it has. If their fitness is improved, the ants can deposit the pheromone increment $\Delta\tau_i$ as in (18). Otherwise, no pheromone is left.

$$\tau_i(t+1) = \begin{cases} \tau_i(t) + \Delta\tau_i & \text{if fitness is improved} \\ \tau_i(t) & \text{otherwise} \end{cases} \quad (18)$$

After each generation, the pheromone is updated as:

$$\tau_i(t+1) = (1-\rho)\tau_i(t) \quad (19)$$

where ρ is the pheromone evaporation rate.

The probability for the local ants can be concluded to select a region is proportional to its pheromone trail. On the other hand, the pheromone is affected by the evaporation rate, ant age, and growth of fitness. Thus, this pheromone-based selection mechanism is capable of promoting the solution candidate update, which is certainly suitable for handling the changing environments in optimization. A proposed flow chart of the ESPRIT-ACO algorithm applied for signal parameter estimation is shown in Fig. (2). Data is obtained by measuring the complex responses of the antenna array elements.

5. Simulation Results

The performance of the ESPRIT in DOA estimation by using ACO algorithm is studied in this section. There are several cases simulated using software developed to function under Matlab 7.8 environment. The receiver antennas are supposed to be uniform linear arrays.

For single emitter source, a simulated narrow-band emitter is used with number of sensors (M=12), number of snapshots (N=50) and suppose the emitter signal with 5dB additive noise is impinging on sensors array from azimuth of 60^o degree. When the ESPRIT algorithm is applied give the result for one emitter in direction 60^o degree is 60.4715^o degree but with ACO algorithm will be given the result for one emitter in direction 60^o degree is 60.0192^o as shown in Fig (3).

For two non-coherent emitter sources with the assumptions that two emitter sources with 5dB additive noise is impinging on a sensor array from azimuth of 60^o and 120^o degrees, The ESPRIT gives the result for two emitter sources in direction 60^o and 120^o degrees is (60.3962^o) and (120.4949^o) degrees and (60.0213^o) and (120.0241^o) when it is implemented with ACO algorithm as shown in Fig (4), and it gives the result for two closely spaced emitter sources in direction 60^o and 63^o degrees is (61.3053^o) and (64.2758^o) degrees and with ACO algorithm is (60.1012^o) and

(63.1109^o) as shown in Fig (5). The ESPIRT algorithm will improve its performance at increasing M and N to 20 and 100 respectively as shown in Fig. (6) with (60.0132^o) and (63.0129^o) arrival angles by using ACO algorithm.

For three non-coherent emitter sources, with the same previous assumptions is applied. The ESPRIT gives the result for three emitter sources in direction 40^o, 90^o and 140^o degrees is (40.4207^o), (90.5227^o) and (140.5217^o) degrees and it gives the results by using ACO algorithm is (40.0215^o), (90.0192^o) and (140.0213^o) as shown in Fig (7), and it gives the result for three closely spaced emitter sources in direction 80^o, 83^o and 86^o degrees is (81.5391^o), (84.3173^o) and (87.6197^o) degrees and (80.1201^o), (83.2383^o) and (86.2198^o) with ACO algorithm as shown in Fig (8). But at increasing M and N to 20, 100 respectively are given the results of (80.0305^o), (83.0313^o) and (86.0218^o). It clear that ESPRIT algorithm with ACO succeed in distinguishing between the closely spaced targets in case non-coherent emitter sources with acceptable computing efficiencies compared with other techniques of DOA estimation as shown in Fig. (9). Finally, from the Fig.(10) of case 1 (single emitter source), it is cleared that for higher values of SNR resolving capabilities of ESPRIT-ACO will be more pronounced than lower values of SNR.

6. Conclusions

Many conclusions can be derived in this paper; the most important results can be summarized as follows:

1. The ACO succeeds in giving reliable results of DOA-ESPRIT without the need of any spectral search for DOA angles.
2. The efficiency of the ESPIRT-ACO algorithm increases with the increasing number of sensors (M) and number of snapshots (N). It is evident that using more sensors (M) and snapshots (N) improves there solution of the algorithm in detecting the incoming signals as shown in Figures (6, 9).
3. The ESPRIT-ACO algorithm achieves accurate DOA estimates without full knowledge of antenna array response.
4. The ESPRIT-ACO algorithm reduces the computation time and it presents low computational complexity in comparison to other DOA methods.
5. With higher values of SNR, the performance of ESPRIT-ACO algorithm will be better than lower values of SNR as shown in Fig. (10).

References

[1] F. Gao and A. B. Gershman "A Generalized ESPRIT Approach to Direction-of-Arrival Estimation" *IEEE Trans. on Signal Processing*, vol. 12, no. 3, pp. 254-257, 2005.

[2] T. N. Ferreira, S. L. Netto and S. R. Paulo, "Covariance Based Direction of Arrival Estimation With Real Structures*" IEEE Trans. on Signal Processing*, vol.15, pp.757-760, 2008.

[3] Y. Xue, J. Wang, and X. Song," Application of Multiresolution Analysis to Diection-of-Arrival Estimation" *International Journal*

of Information and System Sciences, vol. 1, no. 2, pp. 120–136, 2005.

[4] D. Karaboga, K. Guney, and A. Akdagli, "Antenna Array Pattern Nulling by Controlling Both The Amplitude And Phase Using Modified Touring Ant Colony Optimization Algorithm," *Int. J. Electron.*, vol. 91, pp. 241–251, 2004.

[5] W. P. Liao and F. L. Chu, "Array Pattern Nulling by Phase And Position Perturbations With The Use of The Genetic Algorithm," *Microwave Opt. Technol. Lett.*, vol. 15, pp. 251–256, 1997.

[6] S. Yang, Y. B. Gan, and A. Qing, "Antenna Array Pattern Using a Differential Evolution Algorithm," *Int. J. RF Microwave Computer Aided. Eng.*, vol. 14, pp. 57–63, 2004.

[7] A. Colorni, M. Dorigo, and V. Maniezzo, "Distributed Optimization by Ant Colonies, Proceedings of ECAL91", *European Conference on Artificial Life*, Elsevier Publishing, Amsterdam, 1991.

[8] M. Dorigo, V. Maniezzo, and A. Colorni, *The Ant System: An Autocatalytic Optimizing Process*, Technical Report TR91-016, Politecnico di Milano, 1991.

[9] F. Campelo, F. G. Guimaraes, H. Igarashi, and J. A. Ramirez, "A Clonal Selection Algorithm for Optimization in Electromagnetics," *IEEE Trans. Magnetics*, vol. 41, pp. 1736–1739, 2005.

[10] B. Babayigit, A. Akdagli, and K. Guney, "Ant Clone Selection Algorithm For Null Synthesizing of Linear Antenna Arrays By Amplitude Control," *Journal of Electromagnetic Waves and Application*, vol. 20, pp. 1007–1020, 2006.

[11] A. Akdagli, K. Guney, and B. Babayigit, "Clonal Selection Algorithm For Design of Reconfigurable Antenna Array With Discrete Phase Shifters," *Journal of Electromagnetic Waves and Application*, Vol. 21, pp. 215–227, 2007.

[12] S. Das, B. Natarajan, D. Stevens, and P. Koduru, "Multiobjective And Constrained Optimization For DS-CDMA Code Design on The Clonal Selection Principle," *Applied Soft Computing*, vol. 8, pp. 788–797, 2008.

[13] B. Ottersten, M. Viberg, and T. Kailath ''Performance Analysis of the Total Least Squares ESPRIT algorithm'', *IEEE Trans. on Signal Processing*, vol.39, pp.1122-1135, 1991.

[14] K. H. Huarng, and C. C. Yeh ''A Unitary Transformation Method for Angle -of- Arrival Estimation'', *IEEE Trans. on Signal Processing*, vol.39, pp.975-977, 1991.

[15] M. D. Zoltowski, M. Haardt, and G.P .Mathews ''Closed-form 2-D Angle Estimation with Rectangular Arrays in Element Space or Beamspace via Unitary ESPRIT'', *IEEE Trans. on Signal Processing*, vol.44, pp. 316-328, 1996.

[16] M. Dorigo, M. Birattari, and T. Stutzle, "Ant colony optimization", *IEEE Computational Intelligence Magazine*, vol. 1, no. 4, pp. 28-39, 2006.

[17] M. Dorigo, V. Maniezzo, and A. Colorni, "Ant System: Optimization By a Colony of Cooperating Agents", *IEEE Transactions on Systems, Man, and*

Cybernetics-Part B, vol. 26, no 1, pp. 29-41, 1996.

[18] C. Blum, "Beam-ACO Hybridizing Ant Colony Optimization With Beam Search: An Application to Open Shop Scheduling", *Computers & Operations Research*, vol. 32, no. 6, pp. 1565-1591, 2005.

[19] K. Socha, M. Sampel, and M. Manfrin, "Ant Algorithms For The University Course Timetabling Problem With Regard to The State of The Art", *Proc. Workshop on Applications of Evolutionary Computing*, pp. 334-345, 2003.

[20] A. P. Engelbrecht, *Fundamentals of Computational Swarm Intelligence*, Chichester, UK:Wiley, 2005.

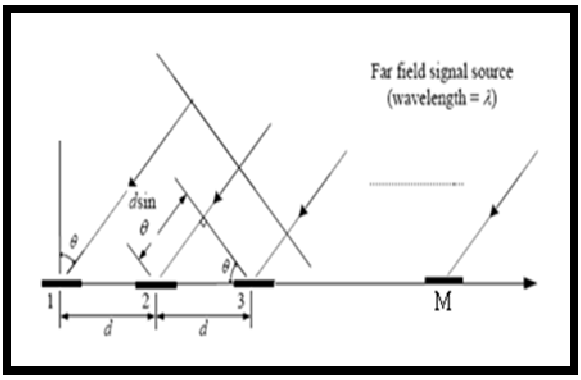

Figure (1): Uniform Linear Array (ULA) and the Direction of Arrival (DOA) problem.

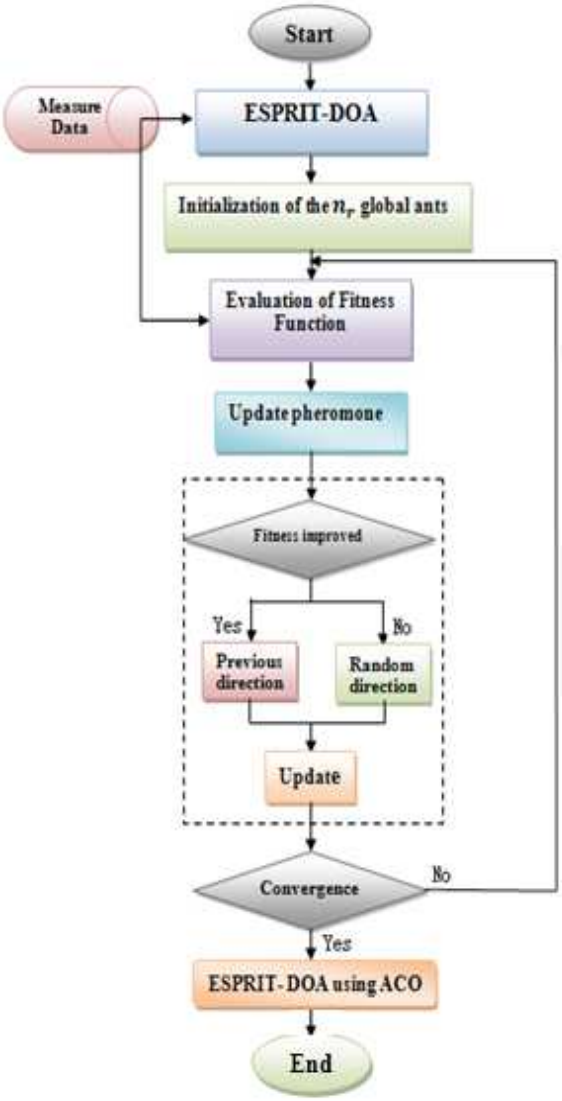

Figure (2) Flow chart of ESPRIT-ACO algorithm.

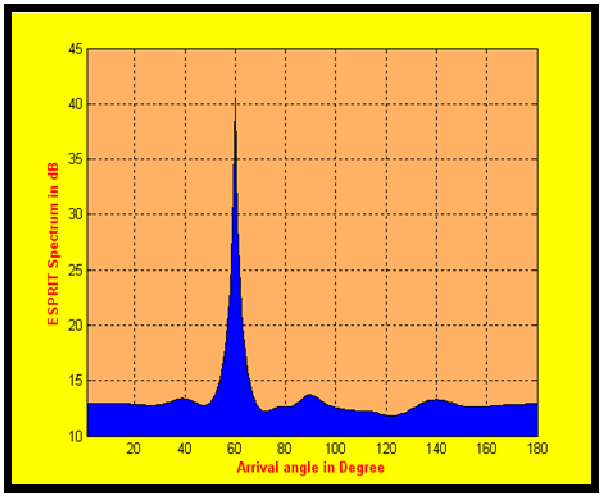

Figure (3): DOA-ESPRIT for single emitter source 60^0 with M=12, N=50 and SNR=5dB.

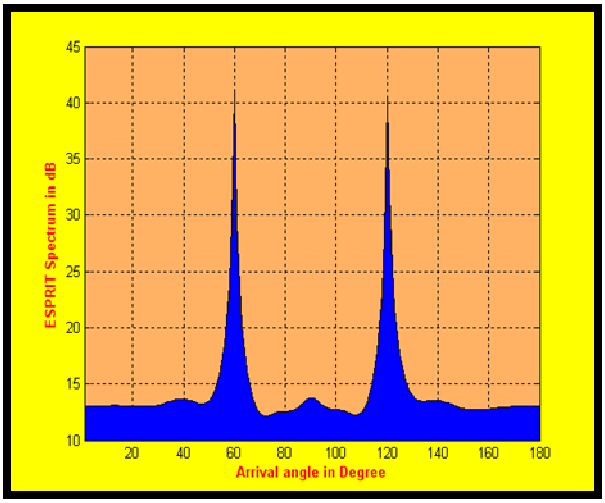

Figure (4): DOA-ESPRIT for two emitter sources 60^0, 120^0 with M=12, N=50 and SNR=5dB.

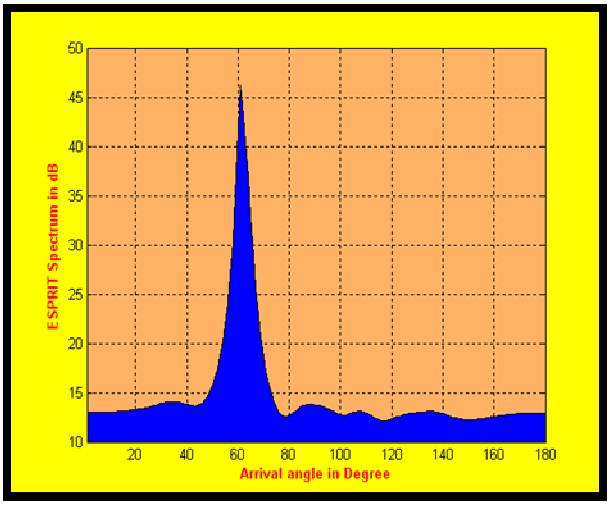

Figure (5): DOA-ESPRIT for two closely spaced emitter sources 60^0, 63^0 with M=12, N=50 and SNR=5dB.

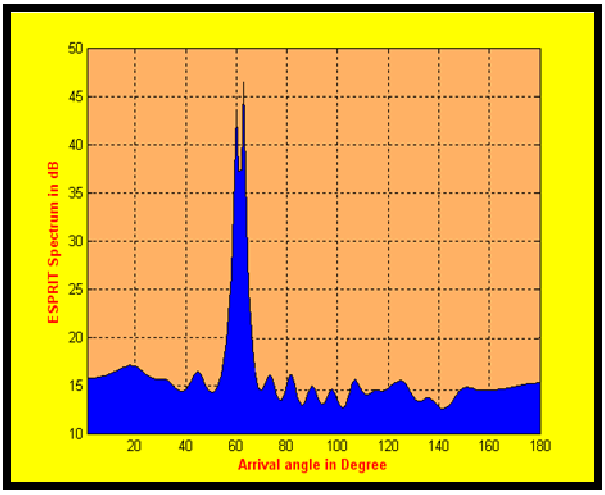

Figure (6): DOA-ESPRIT for two closely spaced emitter sources 60^0, 63^0 with M=20, N=100 and SNR=5dB.

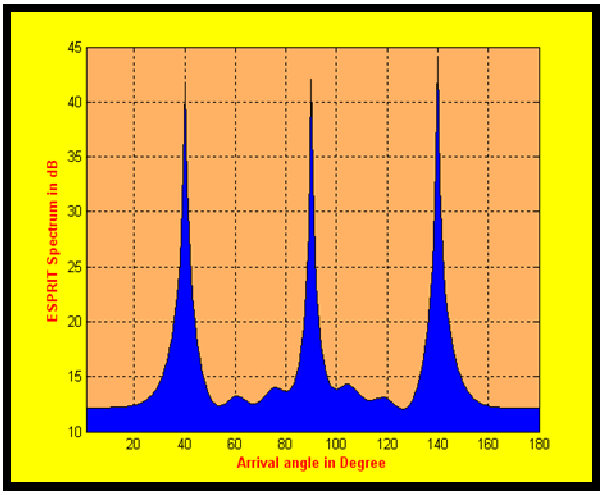

Figure (7): DOA-ESPRIT for three emitter sources. 40^0, 90^0 and 140^0 with M=12, N=50 and SNR=5dB.

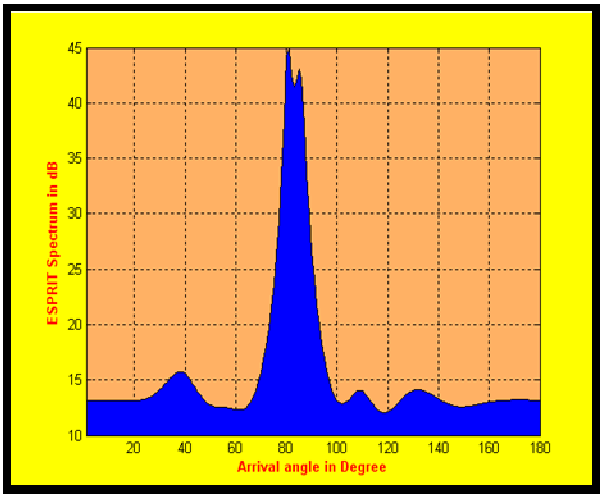

Figure (8): DOA-ESPRIT for three closely spaced emitter sources. 80^0, 83^0 *and* 86^0 with M=12, N=50 and SNR=5dB.

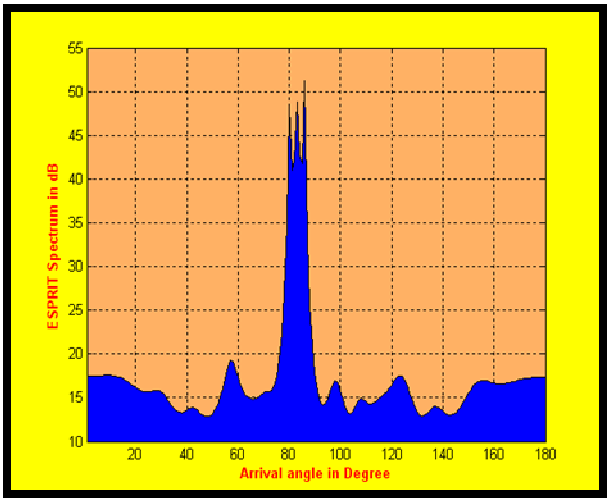

Figure (9): DOA-ESPRIT for three closely spaced emitter sources. 80^0, 83^0 and 86^0 with M=20, N=100 and SNR=5dB.

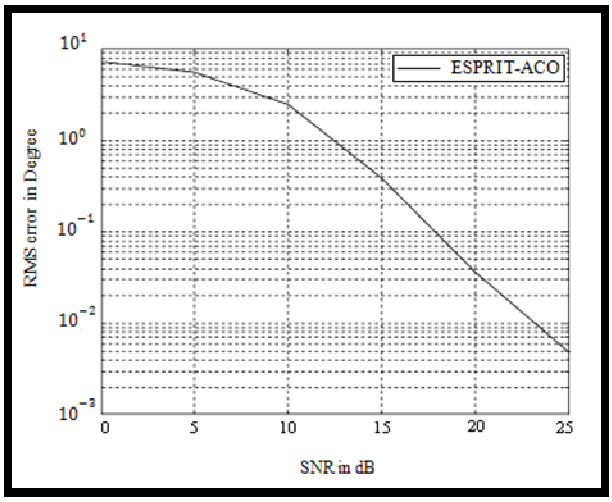

Figure (10) RMS error of the ESPRIT-ACO versus SNR, with M=12, N=50 and V=1.